Conducting Materials Based on Epoxy/Graphene Nanoplatelet Composites With Microwave Absorbing Properties: Effect of the Processing Conditions and Ionic Liquid

Adriana A. Silva[1]*, Raiany Stein[2], Daniela Campos[1], Tamara Indrusiak[3,4], Bluma G. Soares[2,3]* and Guilherme M. O. Barra[5]

[1] Escola de Química, Universidade Federal do Rio de Janeiro, Rio de Janeiro, Brazil, [2] Instituto de Macromoléculas, Universidade Federal do Rio de Janeiro, Rio de Janeiro, Brazil, [3] PEMM-COPPE, Universidade Federal do Rio de Janeiro, Rio de Janeiro, Brazil, [4] Brazilian Army Technological Center, Rio de Janeiro, Brazil, [5] Departamento de Engenharia Mecânica, Universidade Federal de Santa Catarina, Florianopolis, Brazil

Conducting composite materials based on epoxy matrix loaded with graphene nanoplatelets (GNP) were prepared by different procedures using ultrasonication. The dispersions of GNP in a mixture of epoxy/methyl-tetrahydrophthalic anhydride without solvent, resulted in composites with better conductivity, higher storage modulus and higher glass transition temperature than those prepared with solvent assisted procedure, indicating better filler dispersion. The non-covalent functionalization of GNP with the ionic liquid, 1-butyl-3-methyl-imidazolium bis(trifluorosulfonyl) imide (bmim.TFSI) contributed for an increase of the modulus for the systems containing low amount of filler. The electrical conductivity was not influenced by the presence of ionic liquid. Nevertheless, the micro-wave absorption effectiveness in the frequency range of 8-12 GHz (X-band frequency) was improved by the presence of IL mainly for the composites containing 0.9 and 1.5 vol.% of filler. All systems were characterized by low viscosity, comparable to that of neat epoxy resin, thus making easier their application on the development of coatings, conducting adhesives, etc.

Keywords: epoxy resin, graphene nanoplatelets, ionic liquid, electrical conductivity, micro-wave absorption property

INTRODUCTION

Epoxy resins have been widely used as thermosetting matrices for composites and nanocomposites due to their excellent mechanical, thermal and adhesion properties. However, their insulating nature contributes for accumulating static charges during service, which may be dangerous in some situations. Blending epoxy resins with nanoscale carbon-based fillers is considered a promising approach for developing multi-functional thermosetting materials with outstanding mechanical performance and electrical properties, thus enlarging their field of applications as antistatic coatings, conducting adhesives, sensors, electromagnetic interference shielding materials

for electronic devices, etc. Among these fillers, carbon nanotubes (CNT) are nowadays the most studied conductive filler for this purpose, due to their high thermal and electrical conductivity, as well as high aspect ratio, thus contributing for the development of new conducting composites with low percolation threshold, i.e., low amount of filler to attain good level of conductivity for specific purposes (Ma et al., 2010; Sahoo et al., 2010). As the main drawbacks, CNT is still expensive and also induces significant increase in viscosity of the epoxy dispersion, which limits the amount of filler that can be compounded.

Recently, graphene nanoplatelets (GNP) appeared as an alternative for producing conducting polymeric materials due to their excellent thermal, mechanical and electrical properties. GNP consists of few stacked graphene layers, easily obtained by exfoliation of low cost and available natural graphite, being less expensive than CNT. Moreover, the viscosity of epoxy/GNP dispersions is usually lower than that observed for epoxy/CNT dispersions (Martin-Gallego et al., 2013). The superior physico-mechanical performance, better processability and increasing availability of expanded graphite (EG) and graphene nanoplatelets (GNP) led to a large research effort in the last decade related to GNP-based composites (Liu et al., 2018). Several reports describe the superior toughness (Tang et al., 2013; Kang et al., 2017; Chakraborty et al., 2018; Hashim and Jumahat, 2019), reinforcement (Yasmin et al., 2006; Chatterjee et al., 2012) and thermal properties (Prolongo et al., 2014) of epoxy nanocomposites loaded with different amounts of GNP. This filler also promotes an increase of electrical conductivity. However, the values are usually lower than those observed for CNT-based nanocomposites (Martin-Gallego et al., 2013; Yue et al., 2014). This behavior may be attributed to the great tendency of GNP to agglomerate due to the strong Van der Waals forces and π-π interactions between the graphene sheets, which are favored by its planar structure. Therefore, the preparation and exfoliation of GNP commonly involves the treatment with strong acids, which introduces some defects on the electron π conjugation along the graphene surface and negatively affects its intrinsic conductivity. Thus, a great strategy in this field is to find appropriate conditions to promote better dispersion of GNP within a polymer matrix without disturbing the conjugated structure. This can be achieved by employing appropriate mixing conditions and/or the non-covalent functionalization of GNP. Some works in the literature reported the use of sonication (Corcione and Maffezzoli, 2013; Monti et al., 2013) ball milling procedure (Guo and Chen, 2014) and high shear laminar flow using three roll-mill (Ma et al., 2010; Prolongo et al., 2013), among others.

The use of room temperature ionic liquids has been recently considered as another approach to disperse carbon-based nanomaterials due to the favorable cation-π interactions between the carbon surface and ILs. This strategy has been successfully used in epoxy/CNT systems (Throckmorton et al., 2013; Lopes Pereira and Soares, 2016; Sanes et al., 2016; Soares et al., 2016), and also with some epoxy/GNP networks. For example, Zhang and Park (2019) modified GNP previously treated with atmosphere-pressure plasma with 1-ethyl-3-methylimidazolium chloride (emim.Cl) and obtained epoxy/GNP nanocomposites

with improved thermal conductivity and storage modulus, when compared to those produced with non-functionalized GNP. Hameed et al. (2018) used 40% of 1-butyl-3-methylimidazolium chloride (bmim.Cl) in epoxy resin loaded with different amounts of GNP in order to produce flexible epoxy networks. They observed lower conductivity values when compared with epoxy/IL system. Dermani et al. (2018) also employed bmim.Cl in epoxy formulations modified with graphene oxide nanosheets and observed a significant increase on storage modulus and glass transition temperature. Kowsary and Mohammed (2016) prepared reduced graphene oxide covalently modified with magnetic imidazolium-based ionic liquid and used it as filler in epoxy resin. They obtained composites with good microwave absorbing properties. Throckmorton et al. dispersed GNP in a mixture of epoxy and 1-ethyl-3-methylimidazolium dicyanamide (emim.DCN) using three roll-mill (Throckmorton et al., 2013; Throckmorton and Palmese, 2015) and obtained compositions with outstanding electrical conductivity. In this case, IL exerted the role of curing agent. Guo et al. (2009) studied the effect of bmim.PF$_6$ on the curing behavior of epoxy/graphite composites cured with Jeffamine D230, an aliphatic amine. However, no mention regarding the electrical properties was made. Liu et al. (2013) dispersed GNP with 1-aminopropyl-3-butylimidazolium hexafluorophosphate and used in epoxy system cured with methyl-tetrahydrophthalic anhydride (MTHPA). They observed a better dispersion of GNP with IL and an improvement of modulus. However, the electrical properties were not discussed.

The development of sophisticated electronic equipments and communication devices also originates a type of invisible pollution, known as electromagnetic interference, which can affect the efficient operation of other electronic devices. Therefore, studies involving the development of materials with enhanced electromagnetic interference shielding effectiveness (EMI SE) have increased in interest in several fields of telecommunications and other civil applications. Moreover, such materials find enormous interest in the military research involved on the stealth technology. Conducting composites based on carbon materials have been widely employed as microwave absorbing materials, because of their light-weight and cost-effective characteristics, as well as the ability of being used in different forms as film, plaques or even coatings (Thomassin et al., 2013; Sankaran et al., 2018; Wang et al., 2018). The success of these materials is derived of the ability of the conducting particles dispersed inside a certain polymer matrix in interacting with the electromagnetic wave in the microwave frequency range thus absorbing or reflecting the radiation. There are a lot of publications in the literature related to this theme. Most of them discuss the effectiveness of carbon black- and carbon nanotube as the filler for the development of carbon-based composites with these characteristics. The interest related to epoxy/GNP networks also increased in the last decade due to the several advantages of using GNP as conducting filler, such as, low cost, high surface area and high intrinsic conductivity. Liang et al. (2009) used graphene-based sheets in epoxy matrix and obtained composites with around 21 dB shielding efficiency in the X-band frequency range, when 15 wt.% of filler was employed. Kowsary and Mohammed (2016) obtained a maximum of reflection loss

(attenuation of the EM radiation) of 25 dB at 8.62 GHz by using epoxy composite containing 40 wt.% of reduced graphene oxide covalently modified with ionic liquid bearing magnetic anion. Chhetri et al. (2016) prepared graphene oxide non-covalently functionalized with sulfanilic acid azocromotrop followed by reduction with hydrazine. The epoxy composite containing 0.5 wt.% of the modified RGO presented a EMI SE of 226 dB at a frequency of around 2 GHz.

The aim of the work was to investigate the processing conditions for dispersing commercial GNP within the epoxy matrix cured with anhydride and how these conditions affected the electrical conductivity. This work also highlights the influence of the imidazolium-based ionic liquid on the electrical conductivity, thermal properties and microwave absorbing properties of the corresponding epoxy composites. For this purpose, 1-butyl-3-methyl imidazolium bis(trifluormethylsulfonyl) imide (bmim.TFSI) was chosen as the ionic liquid because of its high thermal stability, good ionic conductivity and hydrophobicity when compared with other ionic liquids, thus improving the miscibility with epoxy systems (Herath et al., 2011).

EXPERIMENTAL SECTION

Materials

Epoxy resin, diglycidyl ether of bisphenol A (DGEBA) (MC 130) (epoxide equivalent weight = 185–192; density = 1.25; viscosity = 12.5 Pa.s) was purchased from Turlock, China and commercialized by Epoxyfiber, Brazil. Methyl-tetrahydrophthalic anhydride (MTHPA) used as hardener (density = 1.20; viscosity = 40-70 mPa.s) and benzyldimethylamine used as accelerator was fabricated by DDChem, Italy, and commercialized by EpoxyFiber, Brazil. Graphene nanoplatelet (GNP) (trade name = xGnP-M-5) (average particle diameter = 5 mm; average thickness = 7 nm; density = 2.17 g/cm^3; surface area =130 m^2/g) was purchased from XG Sciences, Lansing. 1-butyl-3-methyl-imidazolium bis(trifluormethylsulfonyl)imide as the ionic liquid (bmim.TFSI) was purchased from Sigma-Aldrich.

Preparation of Nanocomposites

The studies involving the methodology for the dispersion of GNP into epoxy matrix were performed without ionic liquid. The filler was dispersed in the ER using two different procedures: (Method A) the filler was dispersed in a mixture containing ER and acetone (2:1 by weight) under sonication at 135 W for 15 min, with ice bath to avoid heating of the medium. This operation was repeated four times with intervals of 5 min, to ensure good dispersion. After this step, the solvent was removed under vacuum, the MTHPA as the hardener (80 phr related to the resin) and the catalyst (1 phr) were added and the mixture was poured into silicon molds and cured using the following curing protocol: 2 h at 80°C, 2 h at 120°C, and 1 h at 130°C; (Method B) the filler was dispersed in a mixture containing ER and MTHPA (100:80). The medium was sonicated using similar conditions as in the Method A. Then, the mixture was submitted to vacuum to remove some bubbles. After that, 1 phr of the catalyst was added and the mixture was poured into silicon molds and cured with

similar protocol as that mentioned before. The amount of the filler was designed as vol. %. The conversion from wt.% to vol.% was performed by using the density values of each component in the blend.

For the studies related to the effect of ionic liquid on the main properties of the ER/GNP nanocomposites, the GNP was previously modified with different ILs by grinding both components in a mortar for about 20 min. Afterwards, the resulting black paste was dispersed in a mixture of ER/MTHPA using Method B (without acetone).

Characterization

Scanning electron microscopy was performed on a TESCAN (Vega 3 model) at 20 kV. The samples were fractured and coated with thin layer of gold before analysis.

The AC electrical conductivity (σ_{AC}) was measured in a frequency range from 0.1 Hz to 10 MHz using a Solartron SI 1260 gain phase analyzer interfaced to a Solartron 1296 dielectric interface. The measurements were made at 25°C, using electrodes with 25 mm diameter and oscillating voltage of 100 mV. Samples of 1 mm thickness were prepared.

Microwave absorbing properties of the composites were measured at a X-band frequency range (8.2–12.4 GHz) using a network analyzer N530L PNA-L from Agilent, equipped with rectangular waveguide. In order to evaluate the reflection loss, a configuration consisting of metal plate fixed to the sample holder was used. This configuration enables measuring only the reflection parameter. A decreasing of this reflection corresponds to the absorbed radiation (Chen et al., 2004). Samples with 2 mm thickness were employed.
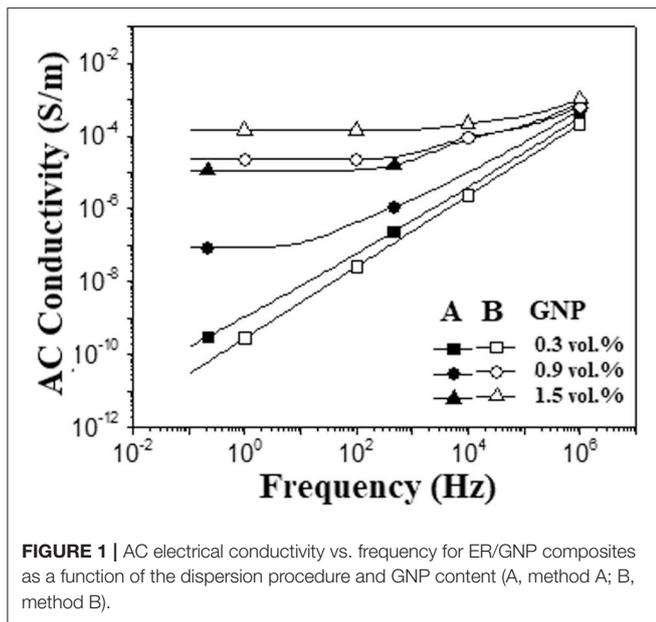
Rheological measurements were carried out with a strain controlled rotational rheometer (DHR, TA Instruments) at 25°C. Nanocomposites samples were loaded between 25 mm parallel plates. They were squeezed into disks ~1 mm thick by slowly lowering the upper plate. The measurements were performed in oscillatory mode in the frequency range from 0.1 to100 rad/s and strain of 0.1%.

Dynamic-mechanical analysis (DMA) was performed in a DMA Q800 from TA Instruments Inc, operating at frequency of 1 Hz, strain of 0.1 % and a heating rate of 3°C/min from 25 to 200°C. Single-cantilever clamp was used in samples with 17 × 12 × 2.5 mm dimensions. The glass transition temperature was taken from the maximum of tan delta peak.

RESULTS AND DISCUSSION

Effect of the Processing Conditions

Two different methodologies were employed to disperse GNP within the epoxy matrix: method A (solvent-assisted procedure) and method B (non-solvent procedure). For method B, it was taken the advantage of the low viscosity of the anhydride-based curing agent, which allows efficient dispersion of the filler in the ER/MTHPA system using ultrasonication, without the solvent assistance. Moreover, the low reactivity of the hardener enables safe dispersion of GNP without premature cure, as the curing only occurs with the addition of the catalyst. **Figure 1** shows the dependence of AC electrical conductivity (σ_{AC}) vs. frequency

FIGURE 1 | AC electrical conductivity vs. frequency for ER/GNP composites as a function of the dispersion procedure and GNP content (A, method A; B, method B).

for the ER/GNP composites prepared by the two different procedures. The composites loaded with 0.55 wt% (0.3 vol.%) of GNP presented a linear dependence of the σ_{AC} with frequency, which is typical of an insulating material. The amount of GNP was too low to allow the formation of a conducting pathway.

Increasing the amount of filler increased the conductivity at low frequency region. The composites with higher amount of filler (0.9 and 1.5 vol %) also presented a DC conductivity plateau at low frequency, which was shifted toward higher frequencies as the amount of filler increased, suggesting the formation of a conductive network. The increase of σ_{AC} beyond a certain frequency indicated that the conducting process turned back to the non-ohmic way (frequency dependent) which is characterized by a hopping-tunneling effect between GNP particles separated by the polymer layer. The composite prepared by method B, loaded with 0.9 vol.% of GNP, displayed σ_{AC} values around three orders of magnitude higher than that prepared by the solvent-assisted procedure (method A). This result suggests that the anhydride used as hardener interacts with GNP and favors the de-agglomeration of the GNP stacks. The better dispersion of GNP endows the GNP particles to touch each other, increasing the conductivity.

The conductivity values found in the present work, prepared by method B, were comparable or even superior to those reported in the literature, as indicated in **Table 1**. Although a comparative study for this system is not reliable due to different nature of the GNP, as well as different hardeners and processing conditions, the present study highlights the effectiveness of the non-solvent processing methodology to achieve good GNP dispersion. These results are interesting for the technological, economical and environmental point of view because it does not use solvent during processing, which also eliminate the solvent withdrawal step under vacuum for several hours or days performing the curing process.

The effect of the processing methodology on the dynamic-mechanical properties of ER/GNP composites was evaluated in terms of storage modulus (E') and tan delta, whose data are summarized in **Table 2**.

The GNP-based composites prepared by both techniques displayed higher E' values than that obtained for the neat epoxy network, except the composite loaded with 0.3 vol.% of GNP and prepared by solvent-assisted method, which presented similar E' value. These results confirm the reinforcing effect of GNP as filler for epoxy network. Similar behavior has been reported in the literature (Saurin et al., 2014). The E' of composites prepared by method A increased as the amount of GNP in the composites increased. Regarding those composites prepared by Method B, the addition of as low as 0.3 vol.% of GNP was enough to increase the modulus in both glassy and rubbery region. Also the addition of 1.5 vol.% of GNP resulted in significant improvement of E' in the glassy region, confirming the better GNP dispersion and higher reinforcing action of the filler by using the non-solvent technique. The glass transition temperature was superior to the neat epoxy network, the difference being more significant for the composites prepared by Method B. For this series, the higher value was obtained by using 0.9 vol.% of GNP. These results can be attributed to the improved interfacial interaction between filler-matrix, probably due to a good interaction between anhydride and GNP during the processing step. Increasing the GNP amount decreased the Tg probably because the formation of GNP aggregates in this higher concentration, which favor the presence of free volume at the filler-matrix interface and a better polymer chain mobility.

The effect of the dispersion methodology on the morphology of ER/GNP composites was evaluated by SEM micrograph, as illustrated in **Figure 2**. The micrographs of the composites prepared by Method A or B are similar, with rough surface. However, it is possible to observe in the samples prepared by method A the presence of agglomerated structures in higher extent, mainly for the samples with higher GNP content (**Figure 2c**).

Effect of Ionic Liquid as Dispersing Agent for GNP

To improve the dispersion of GNP within the epoxy matrix, the filler was previously treated with bmim.TFSI as the ionic liquid to promote a physical interaction between them and facilitate the debundling of the graphene sheets from GNP stacks. The effect of the ionic liquid on the processability of the ER/GNP dispersions was evaluated in terms of complex viscosity (η^*). For this study, the Method B was adopted. Therefore, the measurements were performed in GNP dispersion in the ER/MTHPA mixture. **Figure 3** illustrates the dependence of η^* with frequency for the ER and the corresponding dispersions loaded with 1.5 and 3.0 vol.% of GNP (2.7 and 5.3 wt.%). All systems presented a Newtonian behavior, i.e., the viscosity practically did not change with the frequency. The η^* values of the dispersions were quite similar as that found for neat ER, except that corresponding to the ER/MTHMA dispersion with 3.0 vol.% of GNP/IL, which displayed an increase in viscosity. This behavior suggests some

TABLE 1 | Comparative results of electrical conductivity of epoxy/GNP composites.

GNP amount	Curing agent	Observations	Conductivity (S/m)	References
2 wt.%	triethylenetetramine	Sonication with acetone	10^{-7}	Jovic et al., 2008
2 vol.%	Isophorone diamine		10^{-8}	Corcione and Maffezzoli, 2013
0.63 vol.%	polyamide	Sonication with ethanol	10^{-6}	Zheng et al., 2019
2 wt.%	Methyl-hexahydrophthalic anhydride	Fast dispersion method/sonication without solvent	10^{-4}	Li et al., 2017a
4 wt.%	amine	sonication	10^{-5}	Yue et al., 2014
1.5 vol.%	MTHPA	sonication without solvent	10^{-4}	This work

TABLE 2 | Dynamic-mechanical properties of ER/GNP composites as a function of the processing methodology.

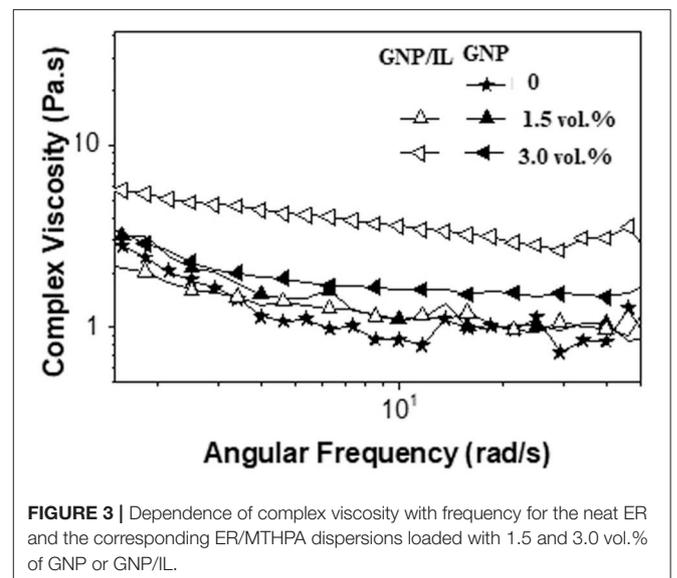| GNP (vol.%)	E' at 25°C (GPa)		E' at 200°C (GPa)		Glass transition temperature (°C)	
	A	B	A	B	A	B
0	1.7		0.013		118	
0.3	1.6	2.0	0.009	0.019	131	142
0.9	1.8	1.8	0.011	0.013	134	141
1.5	2.2	2.7	0.018	0.018	132	133

A, Method A (solvent-assisted method); B, Method B (non-solvent method).
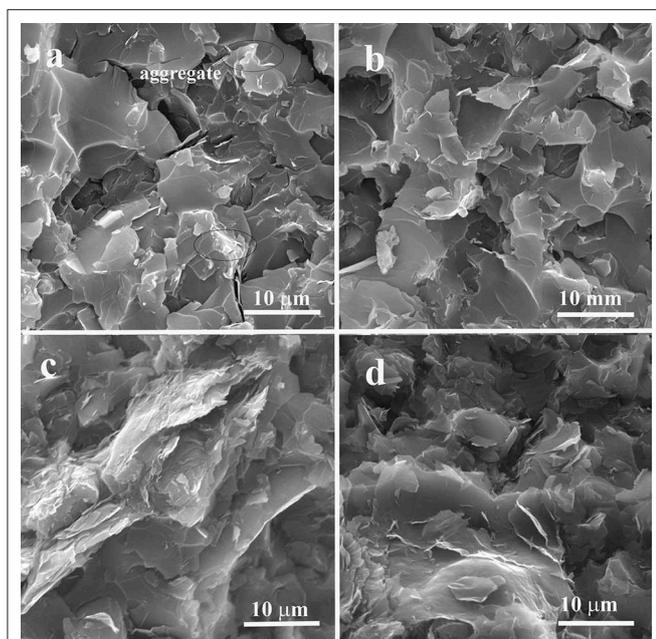
FIGURE 2 | SEM micrographs of ER/GNP loaded with 0.9 vol.% dispersed by **(a)** Method A and **(b)** Method B with 1.5 vol.% of GNP dispersed by **(c)** Method A and **(d)** Method B.

FIGURE 3 | Dependence of complex viscosity with frequency for the neat ER and the corresponding ER/MTHPA dispersions loaded with 1.5 and 3.0 vol.% of GNP or GNP/IL.

TABLE 3 | AC electrical conductivity of epoxy-based composites loaded with different amounts of GNP.

GNP content (vol.%)	AC electrical conductivity at 1 Hz (S/m)	
	Without IL	With 2.2 vol.% of IL
0.3	2.7 ($\pm$0.1) $\times 10^{-10}$	6.0 ($\pm$0.6) $\times 10^{-10}$
0.9	2.0 ($\pm$1.2) $\times 10^{-5}$	9.0 ($\pm$2.9) $\times 10^{-6}$
1.5	1.6 ($\pm$1.0) $\times 10^{-4}$	3.2 ($\pm$3.0) $\times 10^{-5}$
3.0	1.0 ($\pm$0.1) $\times 10^{-4}$	1.0 ($\pm$0.9) $\times 10^{-4}$

improvement of filler-matrix interaction imparted by the IL at the interface. Nevertheless, all dispersions presented low viscosity values due to the presence of the anhydride, which is interesting for processing purpose.

The σ_{AC} values of the composites loaded with GNP and GNP/IL are summarized in **Table 3**, as a function of the GNP content. The values were an average of at least three measurements. Both systems presented a significant transition from an insulator into a semiconductor when the amount of filler increased from 0.3 to 0.9 vol.%. Beyond this concentration,

TABLE 4 | Dynamic-mechanical parameters of ER/GNP composites as a function of the GNP content and the presence of ionic liquid.

GNP content (vol.%)	Storage modulus at 25°C (GPa)		Storage modulus at 190 °C (GPa)		Glass transition temperature (°C)	
	A	B	A	B	A	B
0	1.7		0.011		118	
0.3	2.0	2.0	0.019	0.010	142	126
0.9	1.8	2.3	0.013	0.014	141	129
1.5	2.7	2.6	0.018	0.050	133	146
3.0	2.7	2.3	0.020	0.014	128	132

A, without ionic liquid; B, with 2.2 vol.% of ionic liquid.
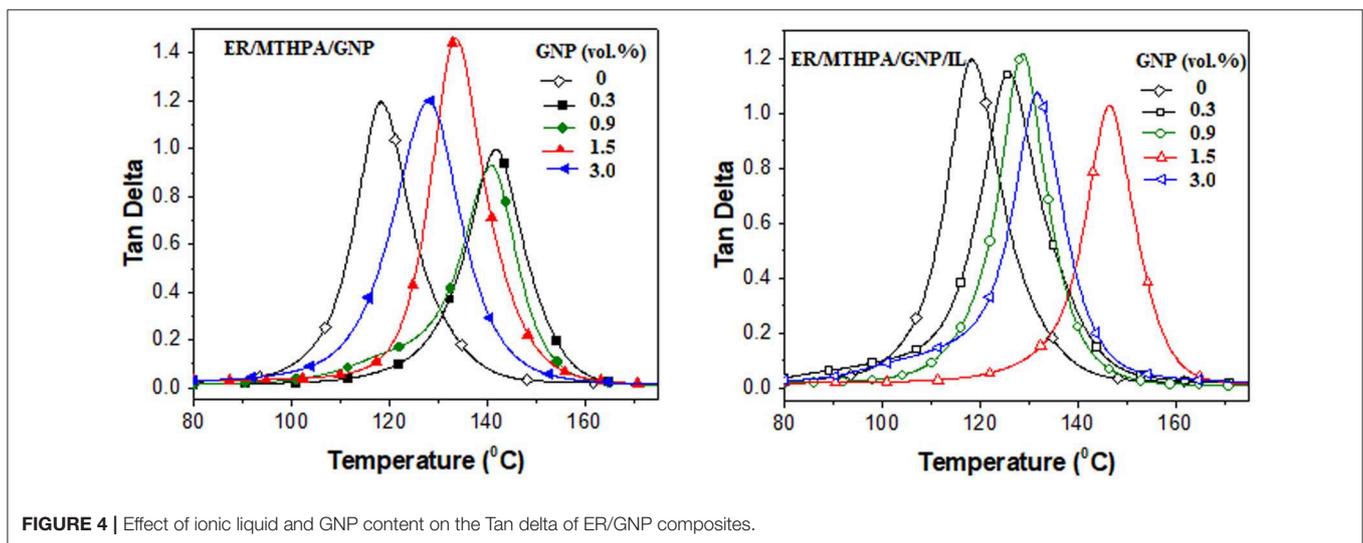
FIGURE 4 | Effect of ionic liquid and GNP content on the Tan delta of ER/GNP composites.

the conductivity slightly increased, probably because of the aggregation of the filler. Similar behavior was reported by Min et al. (2013) for epoxy/GNP composites using similar hardener. The authors observed an increase of the conductivity value at low frequency from the composite loaded with 0.9 vol.% of GNP to that containing 2.7 vol.% of GNP of about one order of magnitude (from 10^{-8} to 10^{-7} S/cm) (Min et al., 2013). Other studies reported that after around 1 vol.% of GNP the conductivity did not change (Yue et al., 2014; Zheng et al., 2019) or even decreased with higher amount of GNP (Yousefi et al., 2013; Li et al., 2017b). According to Zheng et al. (2019) the decrease in the conductivity of the composites with larger GNP loading may be explained by the agglomeration of GNP.

Contrarily to the behavior usually reported for epoxy/CNT functionalized with ionic liquids, the functionalization of GNP with ionic liquid did not exert great influence on the conductivity value of the epoxy-based composites. In fact, a slight decrease of the conductivity was observed with the addition of IL. Zhang and Park (2019) observed an increase of the conductivity of epoxy matrix cured with aromatic amine by using plasma-induced expanded graphite functionalized with 1-ethyl-3-methyl imidazolium chloride.

The different behavior observed in the present work may be due to the different nature of the GNP as well as the different

hardener used to cure the epoxy matrix. One can suggest that the exfoliation of GNP by the IL is a difficult process due to the Van der Waals forces between the graphene sheets, which should be stronger than in the case of CNT due to the planar structure of the sheets, providing more contact points between the sheets. Moreover, the IL at the GNP surface may form a thin insulating layer that prevents direct contact between the conducting filler particles. Xu et al. (2014) observed similar behavior in polypropylene-based composites loaded with carbon nanotube functionalized with imidazolium-type ionic liquid.

The effect of the ionic liquid on the dynamic-mechanical properties of ER/GNP composites was summarized in **Table 4**, as a function of the GNP content. The dependence of the Tan delta with the temperature was also illustrated in **Figure 4**. The E' values of the composites prepared with GNP/IL increased as the amount of filler increased until 1.5 vol.% of filler. Increasing the amount of filler decreased the modulus, probably due some agglomeration of the filler at this concentration (Chhetri et al., 2017). It is interesting to observe that the system loaded with 0.9 vol.% of GNP/IL presented significantly higher E' value than that containing GNP, suggesting a better dispersion of the filler within the epoxy matrix thus forming higher surface area. Moreover, the ionic liquid at the GNP surface should act as an interfacial agent, improving the interfacial adhesion between filler and matrix. The

glass transition temperature was taken as the temperature at the maximum of the tan delta peak. All systems presented higher Tg than the neat epoxy network. Regarding the systems loaded with non-functionalized GNP, the Tg values are higher with low amount of filler (until 0.9 vol.%) and decrease as the amount of filler increase, because of the filler agglomeration phenomenon that occurs with higher filler loading. The formation of aggregates contributes for the presence of free volume at the interface, thus increasing the chain mobility. The decrease of Tg with higher amount of GNP was also reported by Zaman et al. (2011). Regarding the composites loaded with GNP/IL, the Tg increased with the increasing the amount of filler, reaching the maximum value of 146°C at a concentration of GNP corresponding to 1.5 vol.%. After this point, the Tg decreased due to the presence of aggregates. The higher Tg value for the composite loaded with 1.5 vol.% of GNP/IL suggests a good interfacial adhesion between filler and epoxy, thus reducing the mobility of the epoxy chains around the GNP sheet.

Micro-Wave Absorption Property

The effect of ionic liquid on the reflection loss in the X-band frequency range for the ER/GNP composites with a thickness of 2 mm is illustrated in **Figure 5**. The curves present three minimum reflection loss, that, is, maximum of electromagnetic radiation attenuation. For the composites prepared with non-functionalized GNP, the RL is low for the composite containing 0.3 vol.% of GNP and increased when the amount of GNP increased to 0.9 vol.%. After this point, the RL decreased, which can be attributed to an increase of the conductivity. The mobile charge carriers in higher extent interact with EM radiation, thus increasing the reflection phenomenon, higher than absorption. The higher RL value was observed for the composite containing 0.9 vol.%, at 8.75 GHz with RL value of 11.7 dB. The functionalization of the GNP with ionic liquid resulted in composites with higher RL. For the system loaded with 0.3 vol.% of GNP/IL, the minimum RL value was observed at 11.7 GHz with a RL value of 6.9 dB, whereas for the composite containing 0.9 vol.% of GNP/IL, minimum RL values of dB = 9 and 10 dB were observed at−12 and−13 dB, respectively. The composite containing 1.5 vol% presented the better radiation attenuation and this phenomenon corresponded to a frequency of 8.7 GHz. At this point, a RL value of 13.5 dB was obtained, which corresponds to an absorption efficiency of around 96%. These results indicated that the presence of 2.2 vol.% of IL in these composites contributed for a better electromagnetic radiation attenuation, although the conductivity was not varied. This phenomenon may be related to the dispersion of the GNP sheets in the composite. The presence of the IL at the GNP surface provided a better dispersion of the filler. Therefore, the possibility of the interaction of the radiation with the GNP platelets is increased, thus contributing for a better microwave absorption property.

CONCLUSION

Conducting composites based on epoxy matrix containing different proportions of GNP or GNP non-covalently
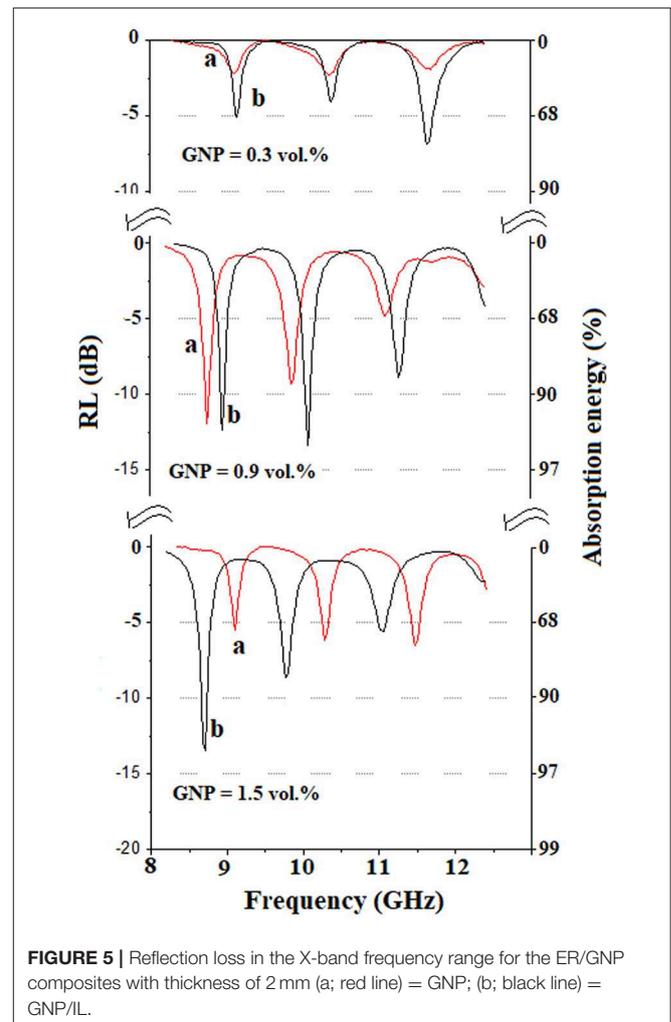
FIGURE 5 | Reflection loss in the X-band frequency range for the ER/GNP composites with thickness of 2 mm (a; red line) = GNP; (b; black line) = GNP/IL.

functionalized with bmim.TFSI as the ionic liquid were prepared in this study. The ER/GNP composites were prepared by two different methodologies: solvent assisted and non-solvent procedure, and cured with MTHPA. The later methodology resulted in higher conductivity values and outstanding storage modulus and glass transition temperature. The functionalization of GNP with 2.2 vol.% of ionic liquid resulted in composites with increased storage modulus when lower amount of GNP/IL was used. Finally, the presence of ionic liquid resulted in better micro-wave absorption properties, which may explained by the better dispersion of the filler. The present work highlights the influence of the ionic liquid as dispersing agent for GNP and opens new possibilities of developing profitable micro-wave absorbing epoxy networks with low viscosity, thus enlarging the field of application, mainly as coating and adhesives.

DATA AVAILABILITY

All datasets generated for this study are included in the manuscript and/or the supplementary files.

AUTHOR CONTRIBUTIONS

RS and DC are undergraduate students of the University, and develop a research project of scientific initiation, and were responsible for preparing the samples for the characterization of the composites. TI contributed with the measurements and interpretation of the absorption analysis of electromagnetic radiation. GB, who has experience in conducting polymers, collaborated in the interpretation of the phenomena of electric conduction of composite materials. BS with extensive experience in composite materials and conductive polymers contributed to the characterization of the mechanical and conductive properties

of the research systems. AS contributed to the interpretation of the mechanical and thermal properties of the composite materials with nanofillers.

REFERENCES

Chakraborty, S., Chakraborty, A. K., Barbezat, M., and Terrasi, G. P. (2018). Interfacial interaction and the fracture toughness (K_{IC}) trends in epoxy nanocomposites filled with functionalized graphene-based fillers. *Polym. Compos.* 39, E2356–E2369. doi: 10.1002/pc.24675

Chatterjee, S., Wang, J. W., Kuo, W. S., Tai, N. H., Salzmann, C., Li, W. L., et al. (2012). Mechanical reinforcement and thermal conductivity in expanded graphene nanoplatelets reinforced epoxy composites. *Chem. Phys. Lett.* 531, 6–10. doi: 10.1016/j.cplett.2012.02.006

Chen, L. F., Ong, C. K., Neo, C. P., Varadan, V. V., and Varadan, V. K. (2004). *Microwave Electronics: Measurements and Materials Characterization*. West Sussex: John Wiley & Sons.

Chhetri, S., Adak, N. C., Samanta, P., Murmu, N. C., and Kuila, T. (2017). Functionalized reduced graphene oxide/epoxy composites with enhanced mechanical properties and thermal stability. *Polym. Test.* 63, 1–11. doi: 10.1016/j.polymertesting.2017.08.005.

Chhetri, S., Samanta, P., Murmu, N. C., Srivastava, S. K., and Kuila, T. (2016). Electromagnetic interference shielding and thermal properties of non-covalently functionalized reduced graphene oxide/epoxy composites. *AIMS Mater. Sci.* 4, 61–74. doi: 10.3934/matersci.2017.1.61.

Corcione, C. E., and Maffezzoli, A. (2013). Transport properties of graphite/epoxy composites: thermal, permeability and dielectric characterization. *Polym. Test.* 32, 880–888. doi: 10.1016/j.polymertesting.2013.03.023

Dermani, A. K., Kowsari, E., Ramezanzadeh, B., and Amini, R. (2018). Screening the effect of graphene oxide nanosheets functionalization with ionic liquid on the mechanical properties of an epoxy coating. *Prog. Org. Coat.* 122, 255–262. doi: 10.1016/j.porgcoat.2018.06.003

Guo, B., Wan, J., Lei, Y., and Jia, D. (2009). Curing behaviour of epoxy resin/graphite composites containing ionic liquid. *J. Phys. D Appl. Phys.* 42, 145307–145315. doi: 10.1088/0022-3727/42/14/145307

Guo, W., and Chen, G. (2014). Fabrication of grapheme/epoxy resin composites with much enhanced thermal conductivity via Ball milling technique. *J. Appl. Polym. Sci.* 131, 40565–40569. doi: 10.1002/app.40565

Hameed, N., Dumée, L. F., Allioux, F. M., Reghat, M., Church, J. S., Naebe, M., et al. (2018). Graphene based room temperature fexible nanocomposites from permanently cross-linked networks. *Nat. Sci. Rep.* 8, 2803-2811. doi: 10.1038/s41598-018-21114-5

Hashim, U. R., and Jumahat, A. (2019). Improved tensile and fracture toughness properties of graphene nanoplatelets filled epoxy polymer via solvent compounding shear milling method. *Mater. Res. Express* 6, 2053–2071. doi: 10.1088/2053-1591/aaeaf0.

Herath, M. B., Hickman, T., Creager, S. E., and DesMarteau, D. D. (2011). A new fluorinated anion for room-temperature ionic liquids. *J. Fluorine Chem.* 132, 52–56. doi: 10.1016/j.jfluchem.2010.11.005

Jovic, N., Dudi,é, D., Montone, A., Antisari, M. V., Mitri,é, M., and Djokovié, V. (2008). Temperature dependence of the electrical conductivity of epoxy/expanded graphite nanosheet composites. *Scripta Mater.* 58, 846–849. doi: 10.1016/j.scriptamat.2007.12.041

Kang, W. S., Rhee, K. Y., and Park, S. J. (2017). Influence of surface energetic of graphene oxide on fracture toughness of epoxy nanocomposites. *Composites Part B*. 114, 175–183. doi: 10.1016/j.compositesb.2017.01.032

Kowsary, E., and Mohammed, M. (2016). Synthesis of reduced and functional graphene oxide with magnetic ionic liquid and its application as an electromagnetic-absorbing coating. *Compos. Sci. Technol.* 126, 106–114. doi: 10.1016/j.compscitech.2016.02.019

Li, A., Zhang, C., and Zhang, Y. F. (2017a). Graphene nanosheets-filled epoxy composites prepared by a fast dispersion method. *J. Appl. Polym. Sci.* 134, 45152–45159. doi: 10.1002/app.45152

Li, Y., Zhang, H., Porwal, H., Huang, Z., Bilotti, E., and Peijs, T. (2017b). Mechanical, electrical and thermal properties of in-situ exfoliated graphene/epoxy nanocomposites. *Composites Part B* 95, 229–236. doi: 10.1016/j.compositesa.2017.01.007

Liang, J., Wang, Y., Huang, Y., Ma, Y., Liu, Z., Cai, J., et al. (2009). Electromagnetic interference shielding of graphene/epoxy composites. *Carbon* 47, 922–925. doi: 10.1016/j.carbon.2008.12.038.

Liu, S., Chevali, V. S., Xu, Z., Hui, D., and Wang, H. (2018). A review of extending performance of epoxy resins using carbon nanomaterials. *Composites Part B* 136, 197–214. doi: 10.1016/j.compositesb.2017.08.0201359-8368

Liu, Y. E., He, C. E., Peng, R., Tang, W., and Yang, Y. (2013). Ionic liquid assisted dispersion of reduced graphene oxide in epoxy composites with improved mechanical properties. *Adv. Mater. Res.* 738, 56–60. doi: 10.4028/www.scientific.net/AMR.738.56

Lopes Pereira, E. C., and Soares, B. G. (2016). Conducting epoxy networks modified with non-covalently functionalized multi-walled carbon nanotube with imidazolium-based ionic liquid. *J. Appl. Polym. Sci.* 133, 43976–43977. doi: 10.1002/app.43976

Ma, P. C., Siddiqui, N., Marom, G., and Kim, J. K. (2010). Dispersion and functionalization of carbon nanotubes for polymer-based nanocomposites: a review. *Composites Part A* 41, 1345–1367. doi: 10.1016/j.compositesa.2010.07.003

Martin-Gallego, M., Bernal, M. M., Hernandez, M., Verdejo, R., and Lopez-Manchado, M. A. (2013). Comparison of filler percolation and mechanical properties in graphene and carbon nanotubes filled epoxy nanocomposites. *Eur. Polym. J.* 49, 1347–1353. doi: 10.1016/j.eurpolymj.2013.02.033

Min, C., Yu, D., Cao, J., Wang, G., and Feng, L. (2013). A graphite nanoplatelet/epoxy composite with high dielectric constant and high thermal conductivity. *Carbon* 55, 116–125. doi: 10.1016/j.carbon.2012.12.017

Monti, M., Rallini, M., Puglia, D., Peponi, L., Torre, L., and Kenny, J. M. (2013). Morphology and electrical properties of graphene-epoxy nanocomposites obtained by different solvent assisted processing methods. *Composites Part A* 46, 166–172. doi: 10.1016/j.compositesa.2012.11.005

Prolongo, S. G., Jimenez-Suarez, A., Moriche, R., and Ureña, A. (2013). In situ processing of epoxy composites reinforced with graphene nanoplatelets. *Compos. Sci. Technol.* 86, 185–191. doi: 10.1016/j.compscitech.2013.06.020

Prolongo, S. G., Jiménez-Suárez, A., Moriche, R., and Ureña, A. (2014). Graphene nanoplatelets thickness and lateral size influence on the morphology and behavior of epoxy composites. *Eur. Polym. J.* 53, 292–301. doi: 10.1016/j.eurpolymj.2014.01.019

Sahoo, N. G., Rana, S., Cho, J. W., Li, L., and Chan, S. H. (2010). Polymer nanocomposites based on functionalized carbon nanotubes. *Prog. Polym. Sci.* 35, 837–867. doi: 10.1016/j.progpolymsci.2010.03.002

Sanes, J., Saurín, N., Carrión, F. J., Ojados, G., and Bermúdez, M. D. (2016). Synergy between single-walled carbon nanotubes and ionic liquids in epoxy resin nanocomposites. *Composites Part B* 105, 149–159. doi: 10.1016/j.compositesb.2016.08.044

Sankaran, S., Deshmukh, K., Ahamed, M. B., and Pasha, S. K. K. (2018). Recent advances in electromagnetic interference shielding properties of metal and carbon filler reinforced flexible polymer compsites: a review. *Composites Part A*. 114, 49–71. doi: 10.1016/j.compositesa.2018.08.006

Saurin, N., Sanes, J., and Bermudez, M. D. (2014). Effect of graphene and ionic liquid additives on the tribological performance of epoxy resin. *Tribol. Lett.* 56, 133–142. doi: 10.1007/s11249-014-0392-2.

Soares, B. G., Riany, N., Silva, A. A., Barra, G. M. O., and Livi, S. (2016). Dual-role of phosphonium – based ionic liquid in epoxy/MWCNT systems: Electric, rheological behavior and electromagnetic interference shielding effectiveness. *Eur. Polym. J.* 84, 77–88. doi: 10.1016/j.eurpolymj.2016.09.016

Tang, L. C., Wan, Y. J., Yan, D., Pei, Y. B., Zhao, L., Li, Y. B., et al. (2013). The effect of graphene dispersion on the mechanical properties of graphene/epoxy nanocomposites. *Carbon* 60, 16–27. doi: 10.1016/j.carbon.2013.03.050

Thomassin, J. M., Jérôme, C., Pardoen, T., Bailly, C., Huynen, I., and Detrembleur, C. (2013). Polymer/carbon based composites as electromagnetic interference (EMI) shielding materials. *Mater. Sci. Eng. R*, 74, 211–232. doi: 10.1016/j.mser.2013.06.001

Throckmorton, J., and Palmese, G. (2015). Direct preparation of few layer graphene epoxy nanocomposites from untreated flake graphite. *Appl. Mater. Interfaces* 7, 14870–14877. doi: 10.1021/acsami.5b03465

Throckmorton, J. A., Watters, A. L., Geng, X., and Palmese, G. R. (2013). Room temperature ionic liquids for epoxy nanocomposite synthesis: direct dispersion and cure. *Compos. Sci, Technol.* 86, 38–44. doi: 10.1016/j.compscitech.2013.06.016

Wang, C., Murugadoss, V., Kong, J., He, Z., Mai, X., Shao, Q., et al. (2018). Overview of carbon nanostructures and nanocomposites for electromagnetic wave shielding. *Carbon* 140, 696–733. doi: 10.1016/j.carbon.2018.09.006

Xu, P., Gui, H., Hu, Y., Bahader, A., and Ding, Y. (2014). Dielectric properties of polypropylene-based nanocomposites with ionic liquid-functionalized multiwalled carbon nanotubes. *J. Electron. Mater.* 43, 2754–2758. doi: 10.1007/s11664-014-3195-1

Yasmin, A., Luo, J. J., and Daniel, I. M. (2006). Processing of expanded graphite reinforced polymer nanocomposites. *Compos. Sci. Technol.* 66, 1182–1189. doi: 10.1016/j.compscitech.2005.10.014

Yousefi, N., Lin, X., Zheng, Q., Shen, X., Pothnis, J. R., Jia, J., et al. (2013). Simultaneous in situ reduction, self-alignment and covalent bonding in graphene oxide/epoxy composites. *Carbon* 59, 406–417. doi: 10.1016/j.carbon.2013.03.034

Yue, L., Pircheraghi, G., Monemian, S. A., and Manas-Zloczower, I. (2014). Epoxy composites with carbon nanotubes and graphene nanoplatelets – dispersion and synergy effects. *Carbon* 78, 268–278. doi: 10.1016/j.carbon.2014.07.003

Zaman, I., Phan, T. T., Kuan, H. C., Meng, Q., La, L. T. B., Luong, L., et al. (2011). Epoxy/graphene platelets nanocomposites with two levels of interface strength. *Polymer* 52, 1603–1611. doi: 10.1016/j.polymer.2011.02.003

Zhang, Y., and Park, S. (2019). Imidazolium-optimized conductive interfaces in multilayer graphene nanoplatelet/epoxy composites for thermal management applications and electroactive devices. *Polymer* 168, 53–60. doi: 10.1016/j.polymer.2019.01.086

Zheng, W., Chen, W. G., Zhao, Q., Ren, S. X., and Fu, Y. Q. (2019). Interfacial structures and mechanisms for strengthening and enhanced conductivity of graphene/epoxy nanocomposites. *Polymer* 163, 171–177. doi: 10.1016/j.polymer.2018.12.055